File name: Supplementary Information
Description: Supplementary figures and supplementary table.

File name: Peer review file
Description:

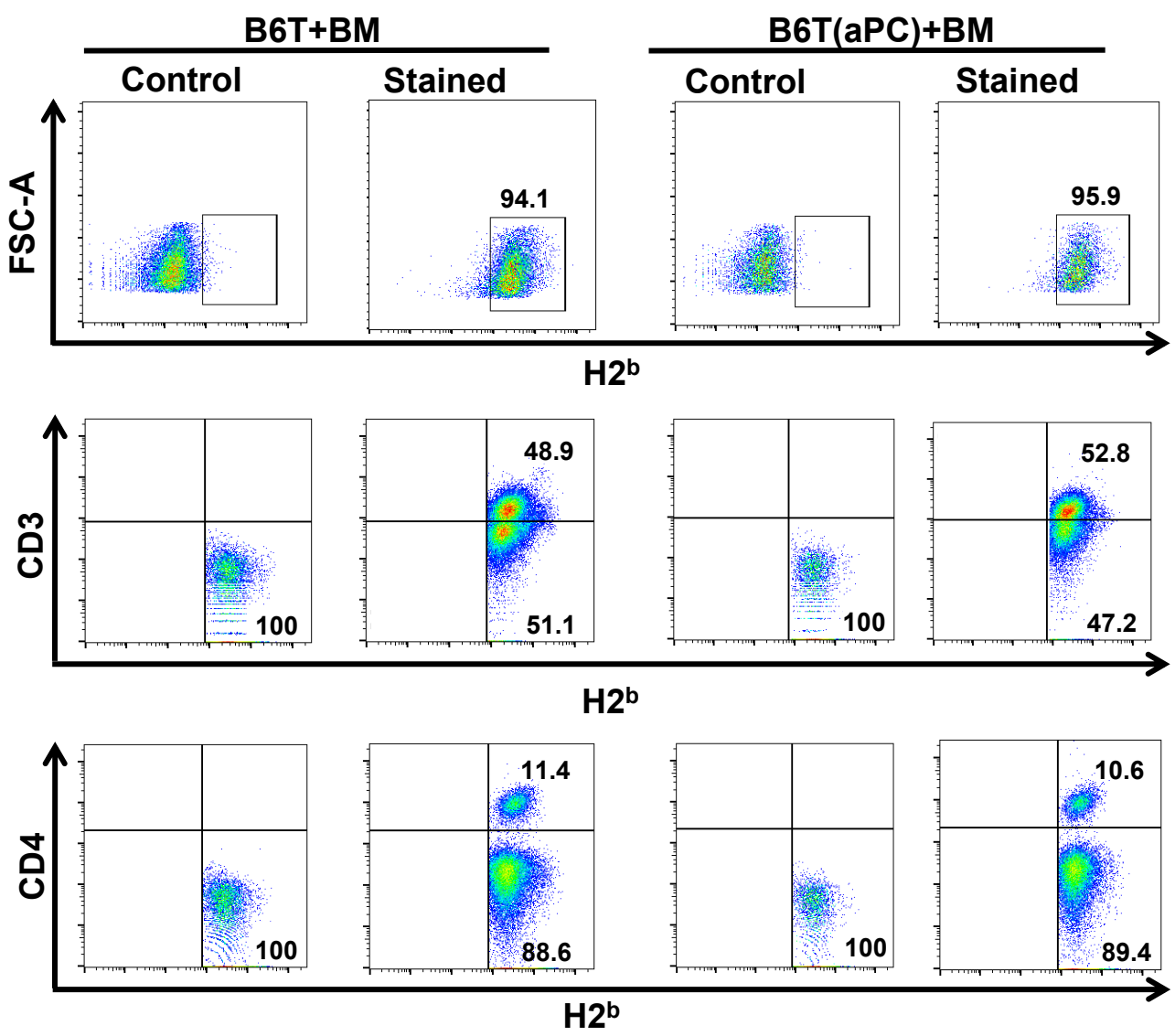


**Supplementary Fig. 1: Engraftment of donor cells ($H2^{b+}$) and donor $CD3^+$ and $CD4^+$ T-cells is not altered by aPC-preincubation of T-cells**

Recipient BALB/c mice were lethally irradiated (11Gy) and transplanted with $5\times10^6$ bone marrow and $0.5\times10^6$ T-cells without (B6T+BM) or with (B6T(aPC)+BM) aPC-preincubation (20nM, 1h, 37°C) from donor C57BL/6 wt mice. Recipient mice were sacrificed on day 3 post transplantation, splenic cells were harvested and stained for $H2^b$, CD3, or CD4 and analysed by flow cytometry. Control: unstained (top) or stained for $H2^b$ only (middle, bottom). Representative FACS images are shown.

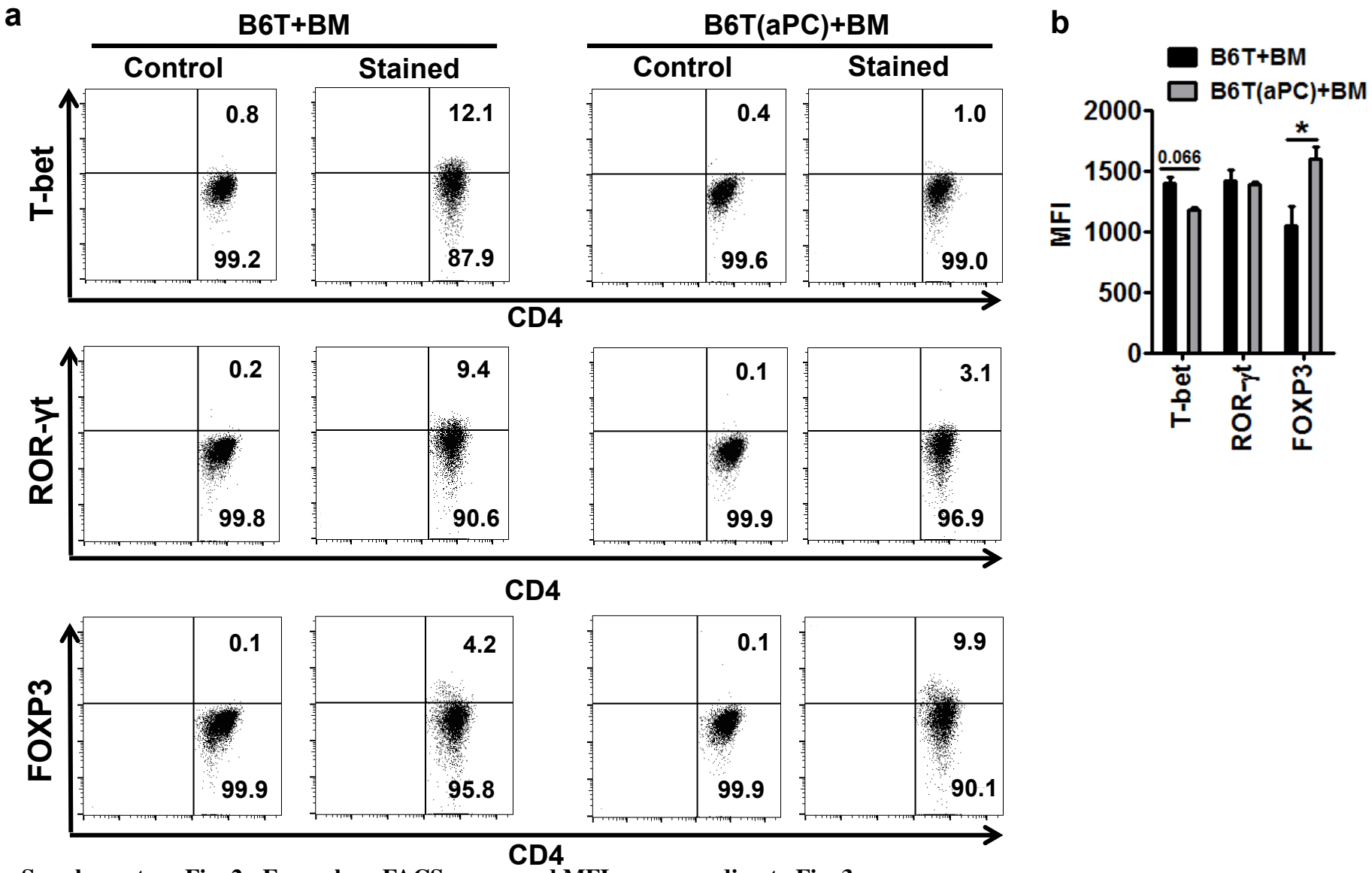


**Supplementary Fig. 2 : Exemplary FACS-scans and MFI corresponding to Fig. 3e**

Recipient BALB/c mice were lethally irradiated (11Gy) and transplanted with $5\times10^6$ bone marrow and $0.5\times10^6$ T-cells without (B6T+BM) or with (B6T(aPC)+BM) aPC-preincubation (20nM, 1h, 37°C) from donor C57BL/6 wt mice. Recipient mice were sacrificed 2 weeks post transplantation, splenic T-cells were harvested and stained for $H2^b$, CD4, T-bet, ROR-γt, or FOXP3 and analysed by flow cytometry. For T-bet, ROR-γt, and FOXP3 cells were gated on $H2^{b+}CD4^+$ cells. Control: stained for $H2^b$ and CD4. Representative FACS images (a) and Mean Fluorescence Intensity (b, MFI, Mean value ± SEM; N=5 each group) are shown; *P<0.05 (b: t-test).

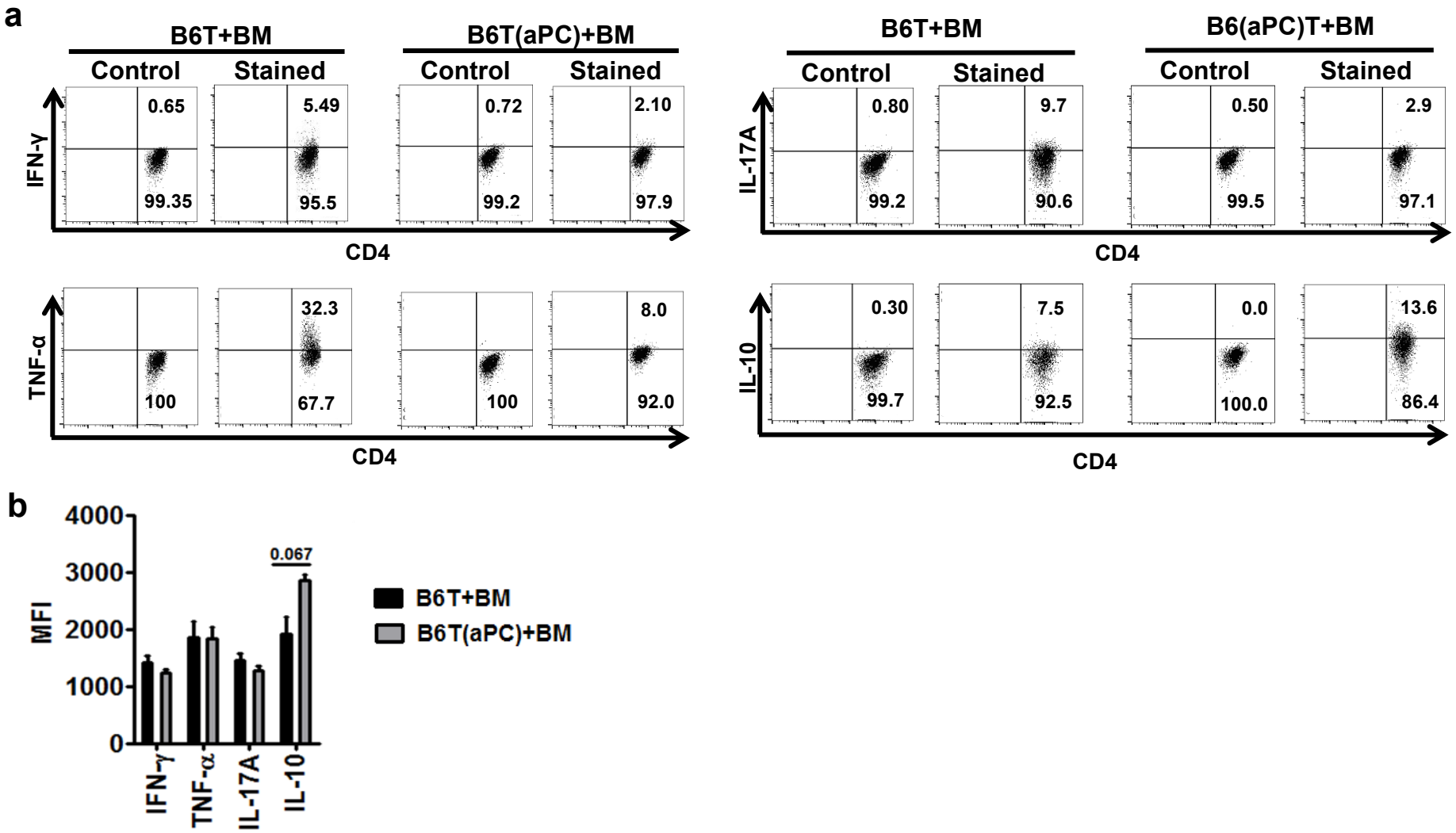


**Supplementary Fig. 3: Exemplary FACS-scans and MFI corresponding to Fig. 3f**

Recipient BALB/c mice were lethally irradiated (11Gy) and transplanted with $5\times10^6$ bone marrow and $0.5\times10^6$ T-cells without (B6T+BM) or with (B6T(aPC)+BM) aPC-preincubation (20nM, 1h, 37°C) from donor C57BL/6 wt mice. Recipient mice were sacrificed 2 weeks post transplantation, splenic T-cells were harvested and stained for $H2^b$, CD4, IFN-γ, TNF-α, IL-17A, or IL-10 and analysed by flow cytometry. For IFN-γ, TNF-α, IL-17A, and IL-10 cells were gated on $H2^{b+}CD4^+$ cells. Control: stained for $H2^b$ and CD4. Representative FACS images (a) and Mean Fluorescence Intensity (b, MFI, Mean value ± SEM; N=5 each group) are shown; (b: t-test).

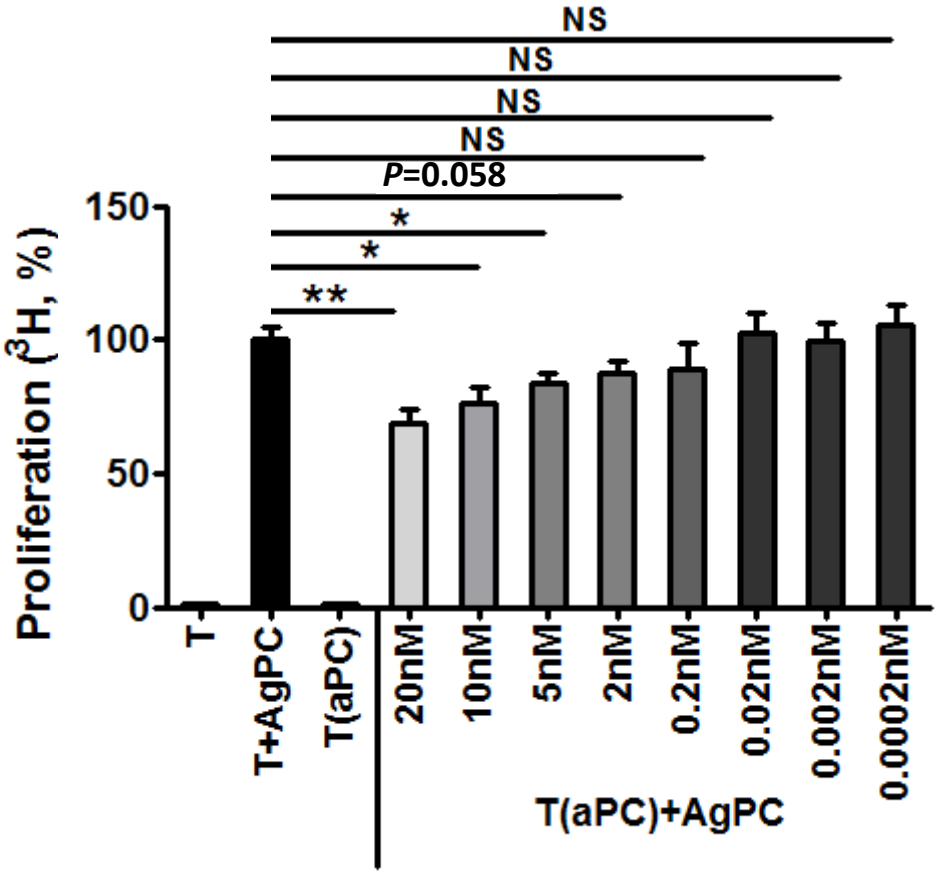


**Supplementary Figure 4: Dose-response of aPC in the MLR**

Following preincubation of human pan-T-cells with various concentrations of aPC (concentration as indicated, preincubation for 1h in AIM V medium) T-cells were co-cultured with irradiated human allogenic antigen-presenting cells for 96h. Allogenic T-cell reactivity was measured by thymidine incorporation during the final 16h. Mean value ± SEM of at least 3 independent experiments, each containing cells from three different donors; **P*<0.05, ***P*<0.01, NS: not significant (t-test).

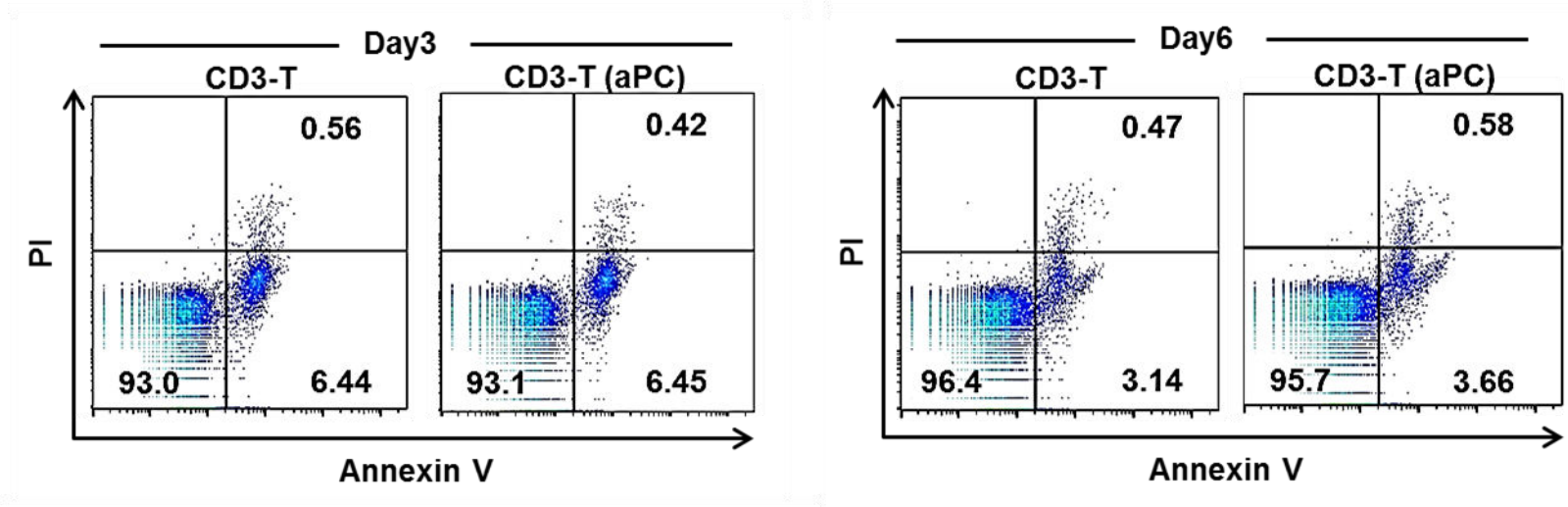


**Supplementary Fig. 5: aPC has no impact on apoptosis in allogenic stimulated human T-cells**
Human T-cells were stimulated with allogenic AgPC for 3 or 6 days and apoptosis was determined by annexin V and PI staining in CD3 T-cells. Representative FACS images of three independent repeat experiments are shown.

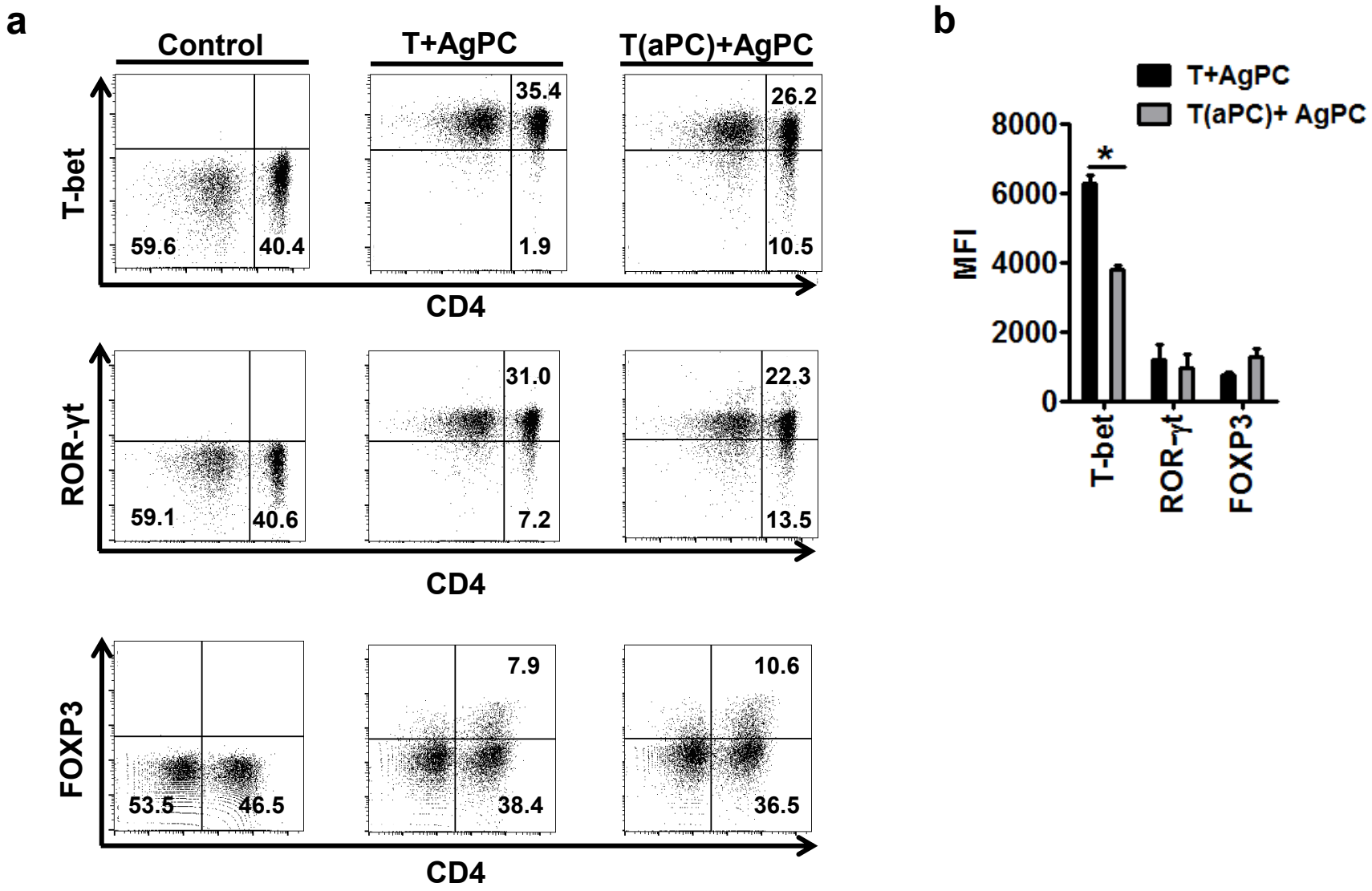


**Supplementary Fig. 6: Exemplary FACS-scans corresponding to Fig. 4d**

aPC-preincubation of human pan T-cells reduces the frequency of $CD4^+$T-$bet^+$ and $CD4^+$ROR-$\gamma t^+$ T-cells, while increasing the frequency of $CD4^+FOXP3^+$ regulatory T-cells, as measured by flow cytometry after 48h of MLR. For T-bet, ROR-γt, and FOXP3 cells were gated on lymphocytes. Control: stained for CD4 only. Representative FACS images (a) and Mean Fluorescence Intensity (b, MFI, Mean value ± SEM; N=5 each group) are shown; *P<0.05 (b: t-test).

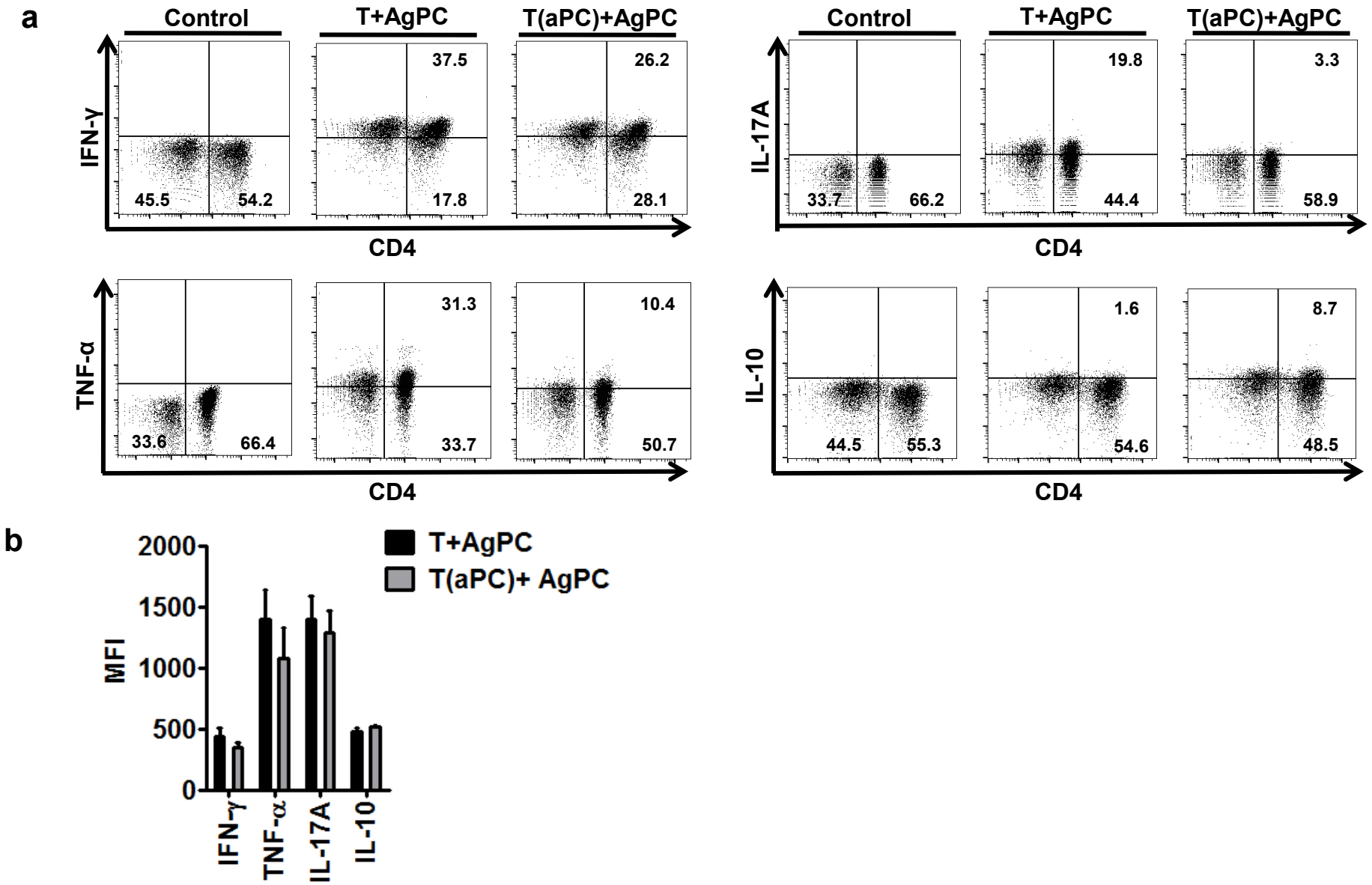


**Supplementary Fig. 7: Exemplary FACS corresponding to Fig. 4e**

aPC-preincubation of human pan T-cells reduces expression of the pro-inflammatory cytokines IFN-γ, TNF-α, and IL-17A, while that of IL-10 is increased as measured by flow cytometry after 48h of MLR. For IFN-γ, TNF-α, IL-17A, or IL-10, cells were gated on lymphocytes. Control: stained for CD4 only. Representative FACS images (a) and Mean Fluorescence Intensity (b, MFI, Mean value ± SEM; N=5 each group) are shown.

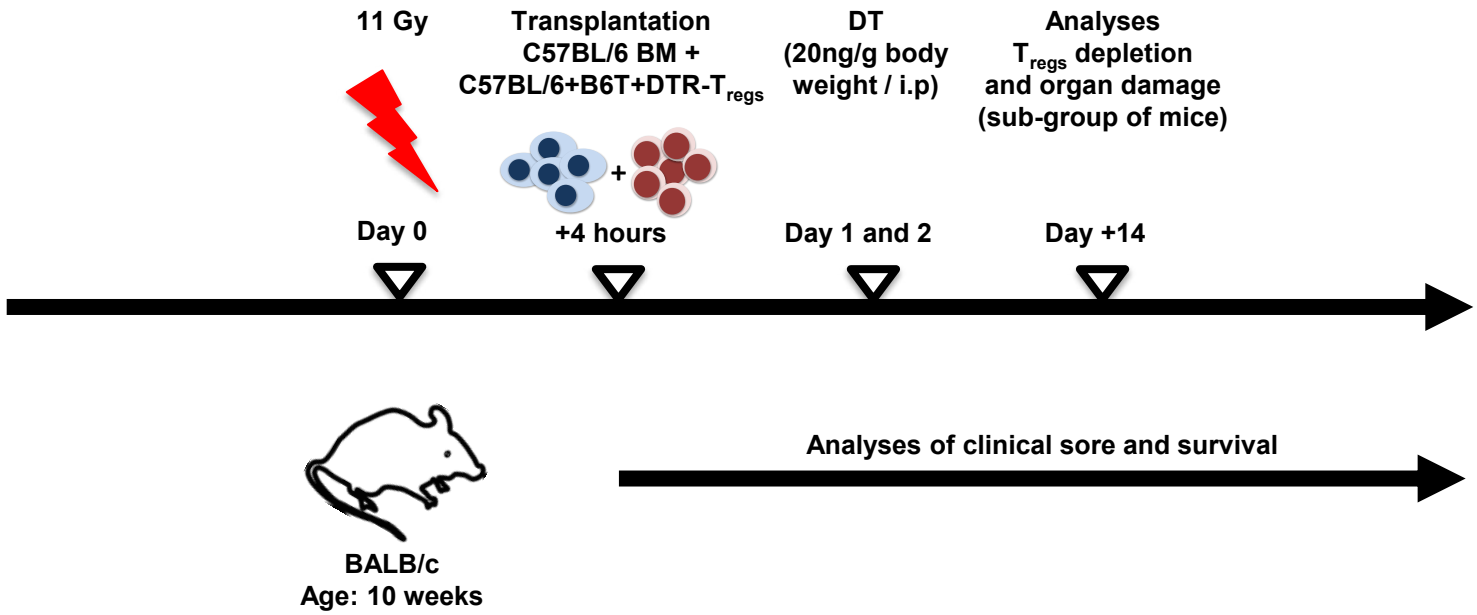


**Supplementary Fig. 8: Scheme presenting experimental approach of transplantation of DTR-$T_{reg}$ in mice.**
Experimental approach for depletion of $T_{regs}$ in mice transplanted with DEREG derived $T_{regs}$. BALB/c mice, age 10 weeks, were irradiated with a single dose (11 Gy). Post-irradiation (after 4h) mice were transplanted with C57BL/6 derived bone marrow cells (5 x $10^6$), C57BL/6 derived T-cells (0.4 x $10^6$) and $T_{regs}$ (0.1 x $10^6$) obtained from DEREG mice expressing the diphtheria toxin receptor (DTR) and eGFP under the control of the FOXP3 promoter. $T_{regs}$ were preincubated with aPC (20 nM, in AIM V medium) or left untreated (only AIM V medium) for 1h. On day 1 and 2 mice were injected with diphtheria toxin (DT, 20ng/g body weight /intraperitoneal injection (i.p)). Depletion of $T_{regs}$ was ascertained on day 14 by isolating splenocytes and determining the frequency of GFP expressing $T_{regs}$ cells in a subgroup of mice. Other mice were continuously monitored and a clinical score to quantitate GvHD severity was generated. See material and methods section for further details.

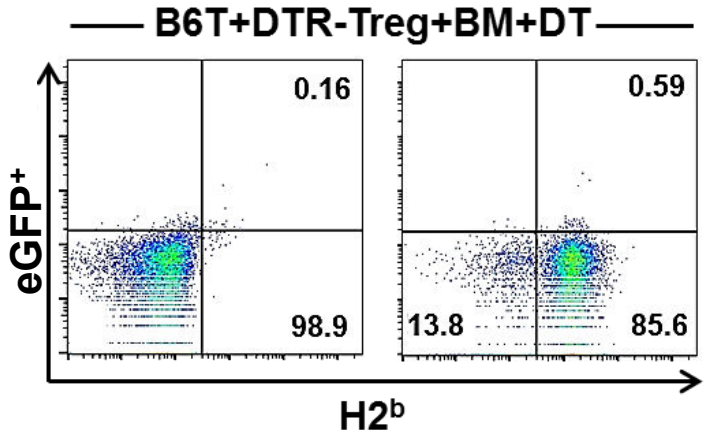


**Supplementary Fig. 9: Depletion of donor GFP$^+$DTR$^+$-T$_{regs}$**

Recipient mice were transplanted with C57BL/6 derived bone marrow cells (5 x $10^6$), C57BL/6 derived T-cells (0.4 x $10^6$) and $T_{regs}$ (0.1 x $10^6$) obtained from DEREG mice on day 0 and injected with DT (20ng/g body weight, i.p.) on day 1 and 2 (B6T+DTR-Treg+BM+DT). Splenic donor cells ($H2^{b+}$) were analysed for GFP$^+$ DTR-Treg in transplanted mice by FACS on day 14. Exemplary FACS images shown (left: $H2^b$ negative control, right: $H2^{b+}$eGFP$^+$ $T_{regs}$).

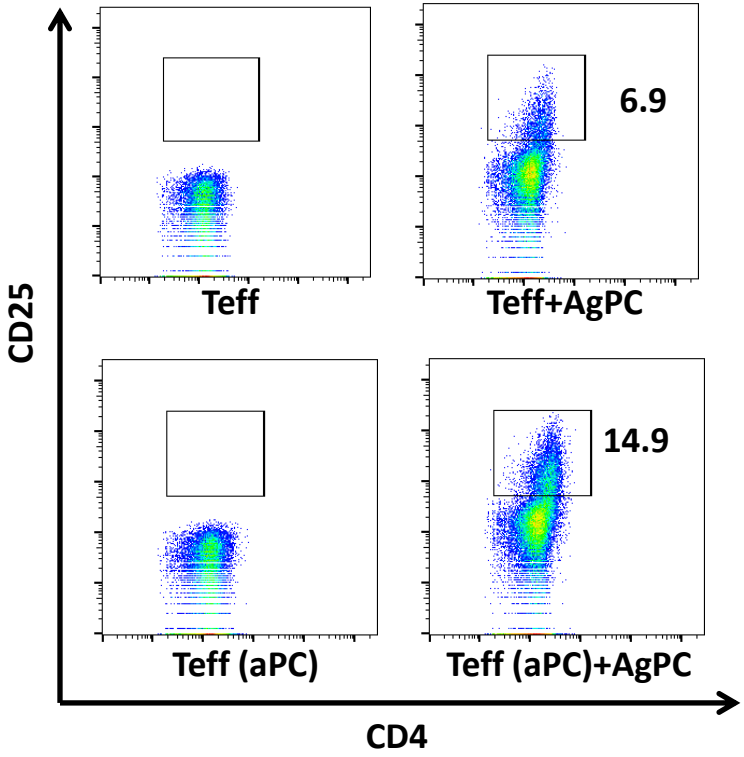


**Supplementary Fig. 10: Exemplary FACS corresponding to Fig 5e**
Preincubation of human effector T-cells ($CD4^+CD25^-$) with aPC induces regulatory cells ($CD4^+CD25^+$). Effector T-cells without ($T_{eff}$) and with ($T_{eff}$(aPC)) aPC-preincubation were stimulated with AgPC for 96h. Cells were measured by FACS and analysed by FlowJo software. Representative FACS images are shown.

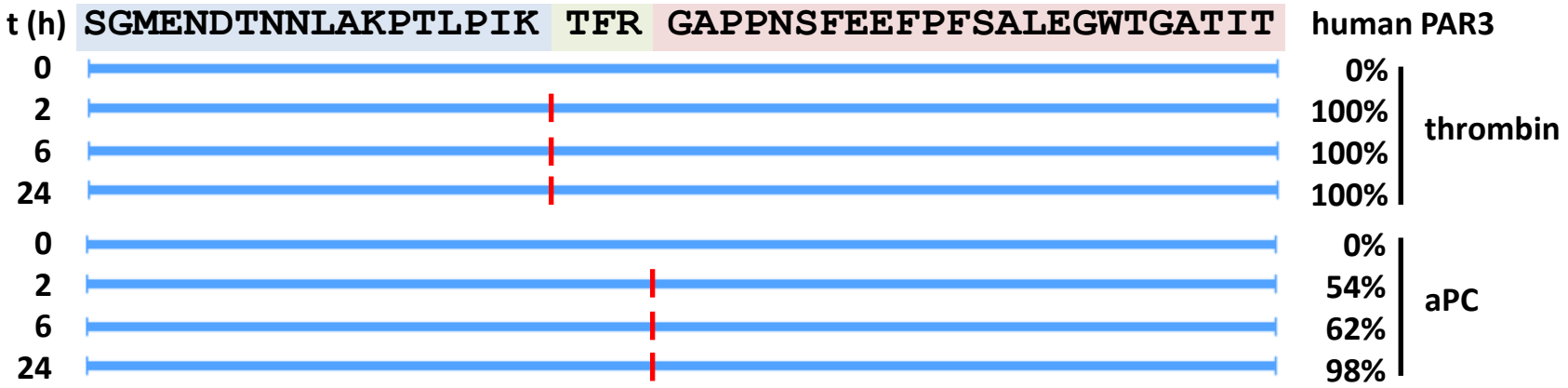


**Supplementary Fig. 11: Summary of human PAR3-N-terminal peptide cleavage analyses.** A peptide derived from the N-terminal end of human PAR3 (sequence shown at the top) was incubated with human thrombin (10 nM) or human aPC (500 nM). Proteolysis was determined at indicated time-points (left, t(h)). Cleavage sites are shown in red lines and estimated cleavage efficiency is shown in percentage (right).

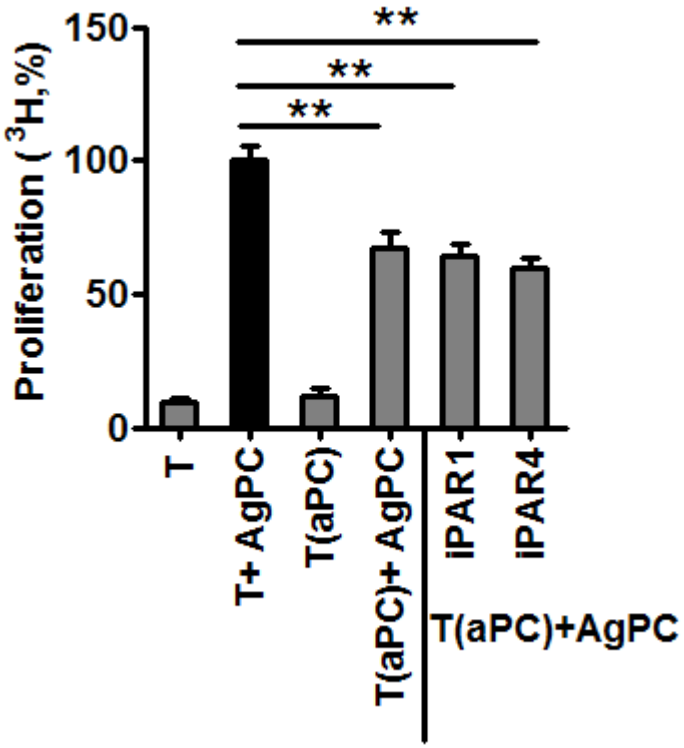


**Supplementary Fig. 12: Inhibitory peptides against PAR1 and PAR4 failed to abolish aPC's effect in the MLR** Preincubation of human peripheral blood T-cells (T) with inhibitory peptides against PAR1 (iPAR1) or PAR4 (iPAR4) prior to aPC-preincubation and MLR does not abrogates aPC's inhibitory effect in regard to T-cell reactivity. Mean value ± SEM); **P<0.01 (t- test).

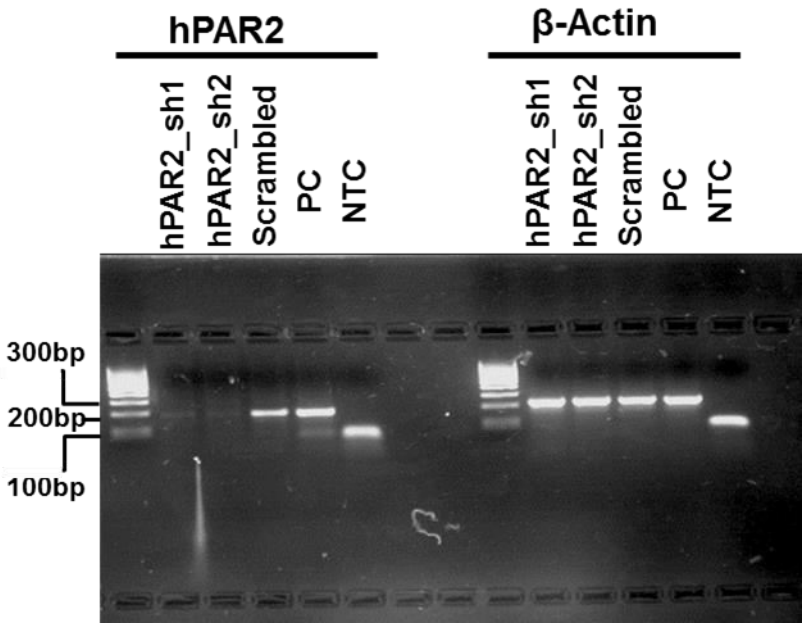


**Supplementary Fig. 13: Knock down of PAR2 in primary human T-cells.** Primary human T-cells were transfected with lentiviral particles mediating expression of two disjunct shRNA (hPAR2_sh1, hPAR2_sh2) against human PAR2 (178bp) or a control shRNA (scrambled). Both shRNAs efficiently suppressed expression of PAR2, while the control shRNA had no effect. Beta actin (β-Actin-227bp) was used as loading control. Exemplary image of an RT-PCR analyses conducted on day 2 after transfection. SM: size marker, PC: positive control (non-transduced human pan-T-cells; NTC: negative control (no reverse transcriptase).

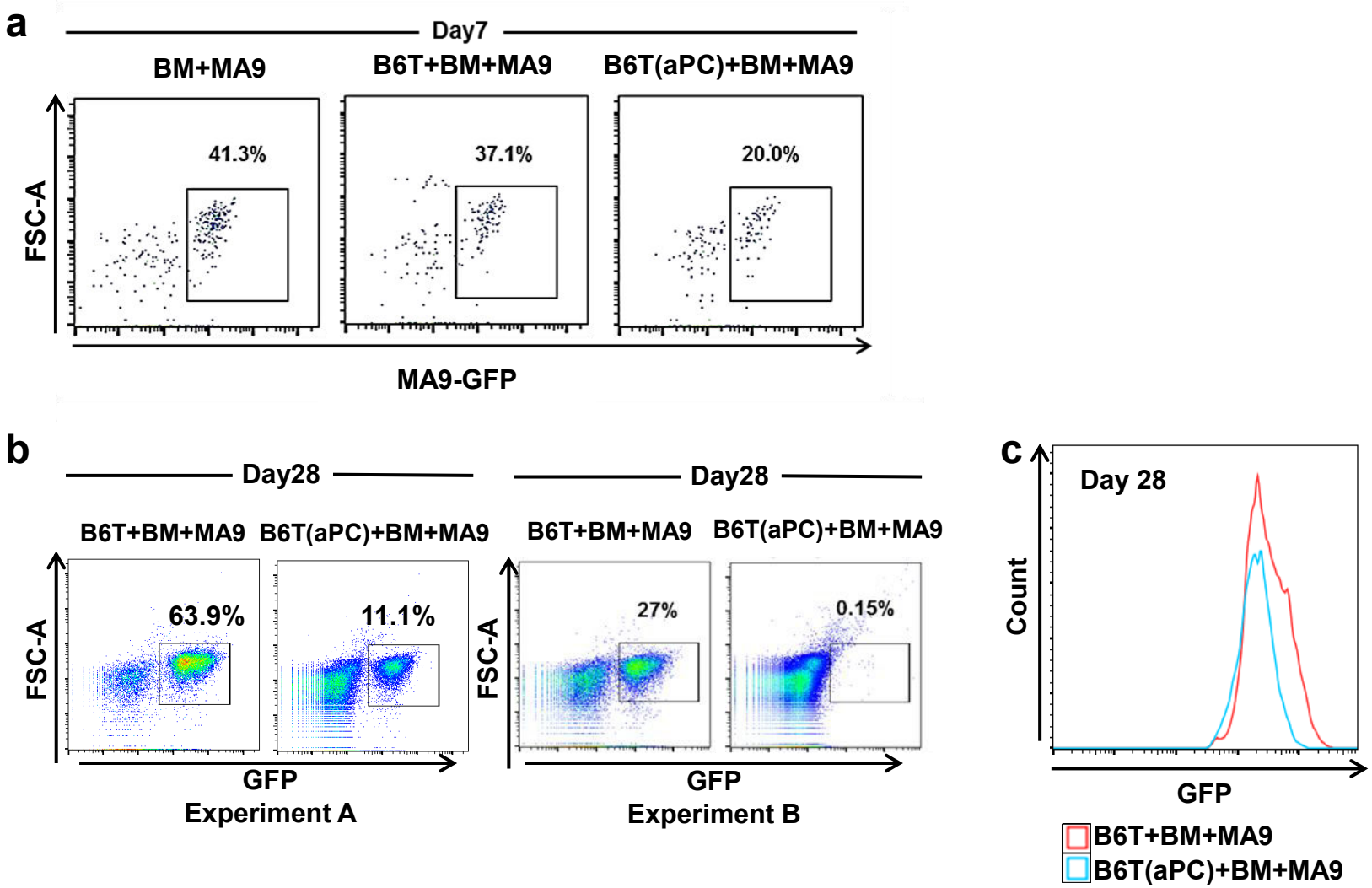


**Supplementary Fig. 14: Exemplary FACS-scans corresponding to Fig. 10b,c**
Lethally irradiated (11Gy) recipient BALB/c mice were transplanted with $5\times10^6$ C57BL/6 derived bone marrow cells, 5000 GFP$^+$MA9 leukemic cells, and $0.5\times10^6$ C57BL/6 T-cells without (B6T+BM+MA9) or with (B6T(aPC)+BM+MA9) aPC-preincubation. In mice transplanted with aPC preincubated T-cells leukemic load (determined by flow cytometry on day 7 (a) and day 28 (b,c) after transplantation in peripheral blood samples) is markedly decreased. Representative FACS images (a,b) and histogram (c) are shown.

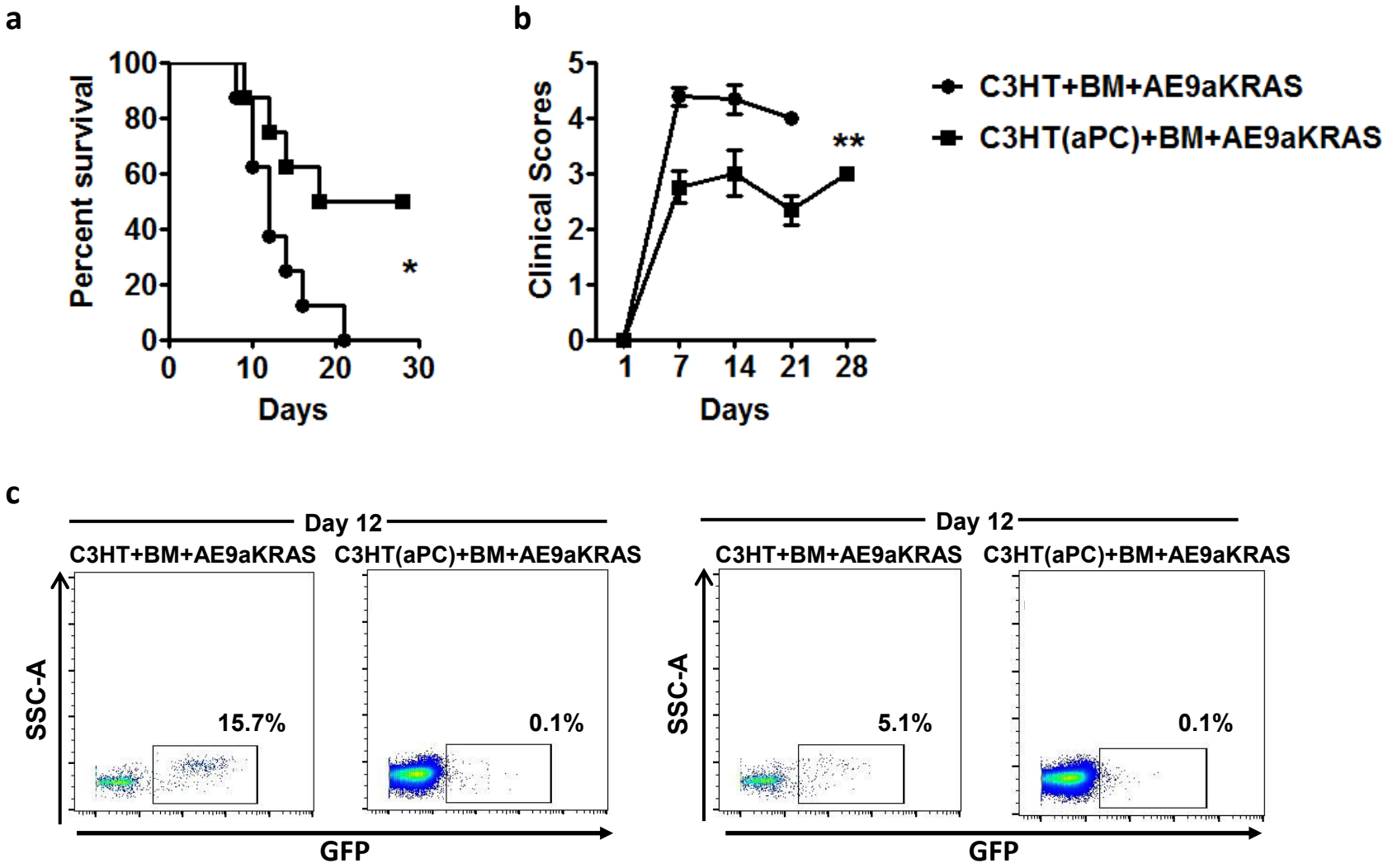


**Supplementary Fig. 15: aPC preincubation of T-cells does not impair GvL effect**

Lethally irradiated (13Gy) recipient C57BL/6 mice were transplanted with $5\times10^6$ C3H derived bone marrow cells, $2\times10^4$ GFP$^+$AE9aKRAS leukemic cells, and $1\times10^6$ C3H T-cells without (C3HT+BM+AE9aKRAS) or with (C3H(aPC)+BM+AE9aKRAS) aPC-preincubation. Survival curve (a) and clinical scores (b) are shown. In mice transplanted with aPC preincubated T-cells leukemic load (determined by flow cytometry on day 12 (c) after transplantation in peripheral blood samples) is markedly decreased. Representative FACS images (c) are shown.. Mean value ± SEM; N=8 each group) are shown; *P<0.05, **P<0.01 (log-rank test).

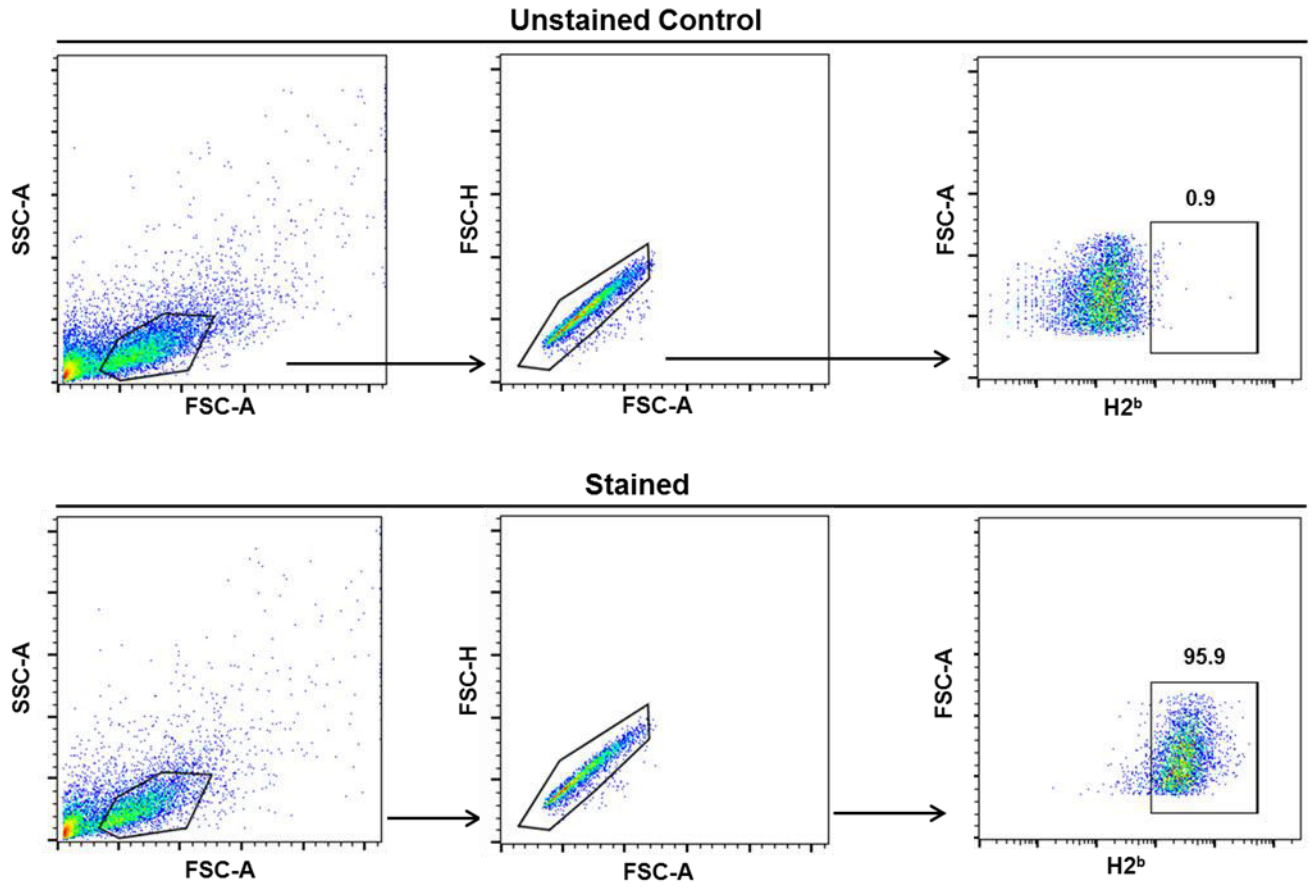


**Supplementary Fig. 16:** Representative gating strategy for unstained control and stained samples corresponding to Supplementary Figure 1 (part 1).

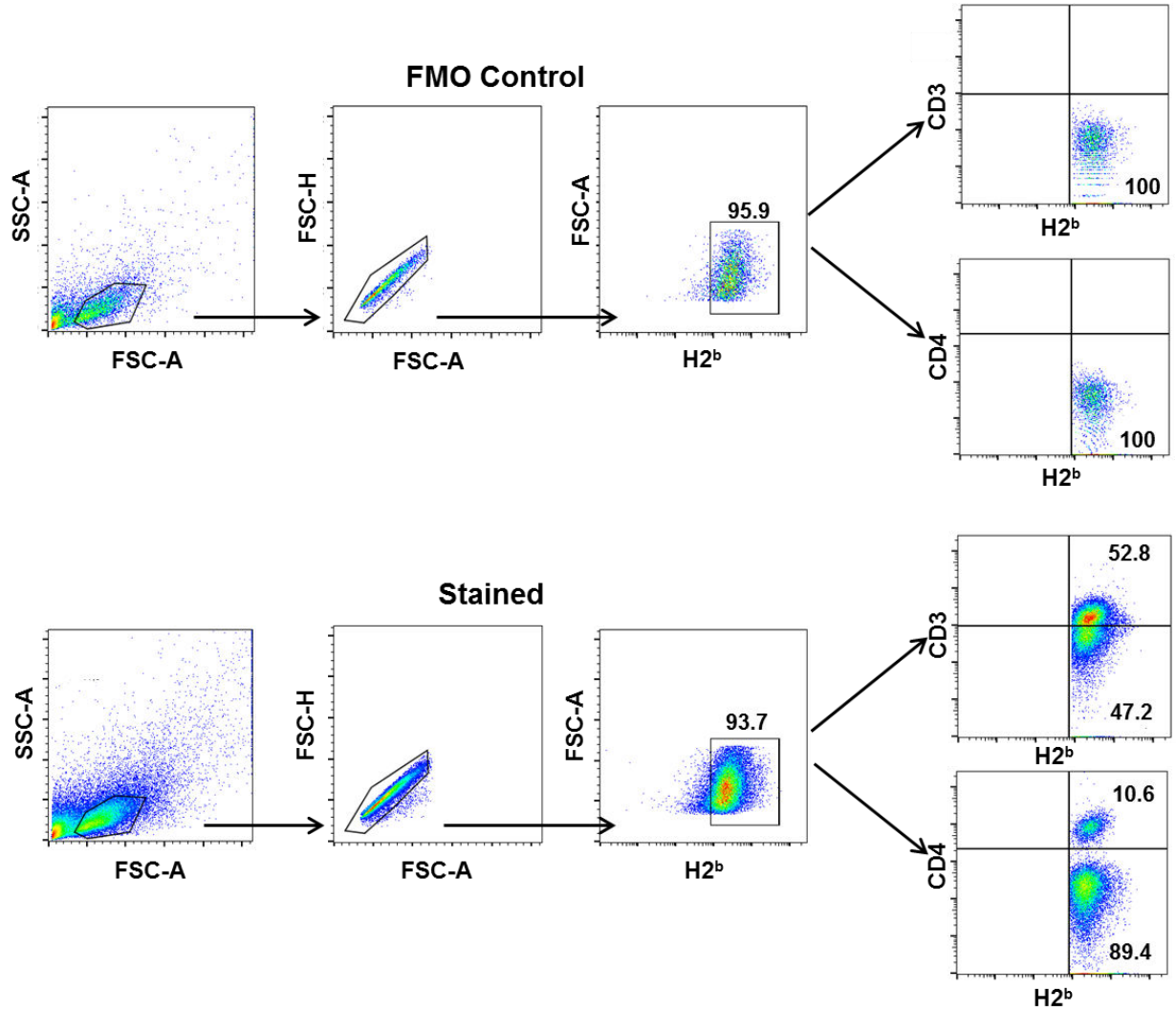


**Supplementary Fig. 17:** Representative gating strategy for FMO control and stained samples corresponding to Supplementary Figure 1 (part 2).

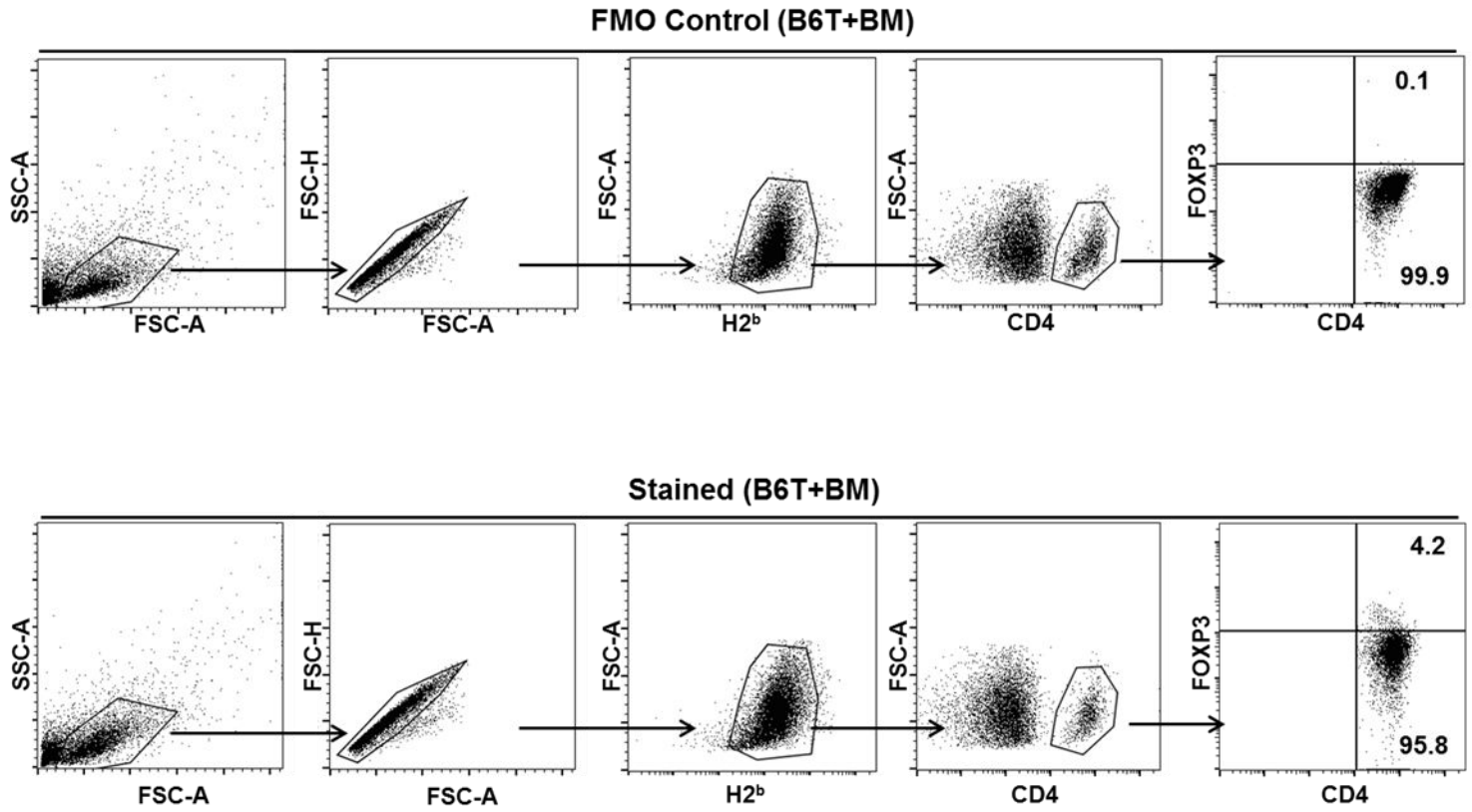


**Supplementary Fig. 18:** Representative gating strategy for FMO control and stained samples corresponding to Supplementary Figure 2.

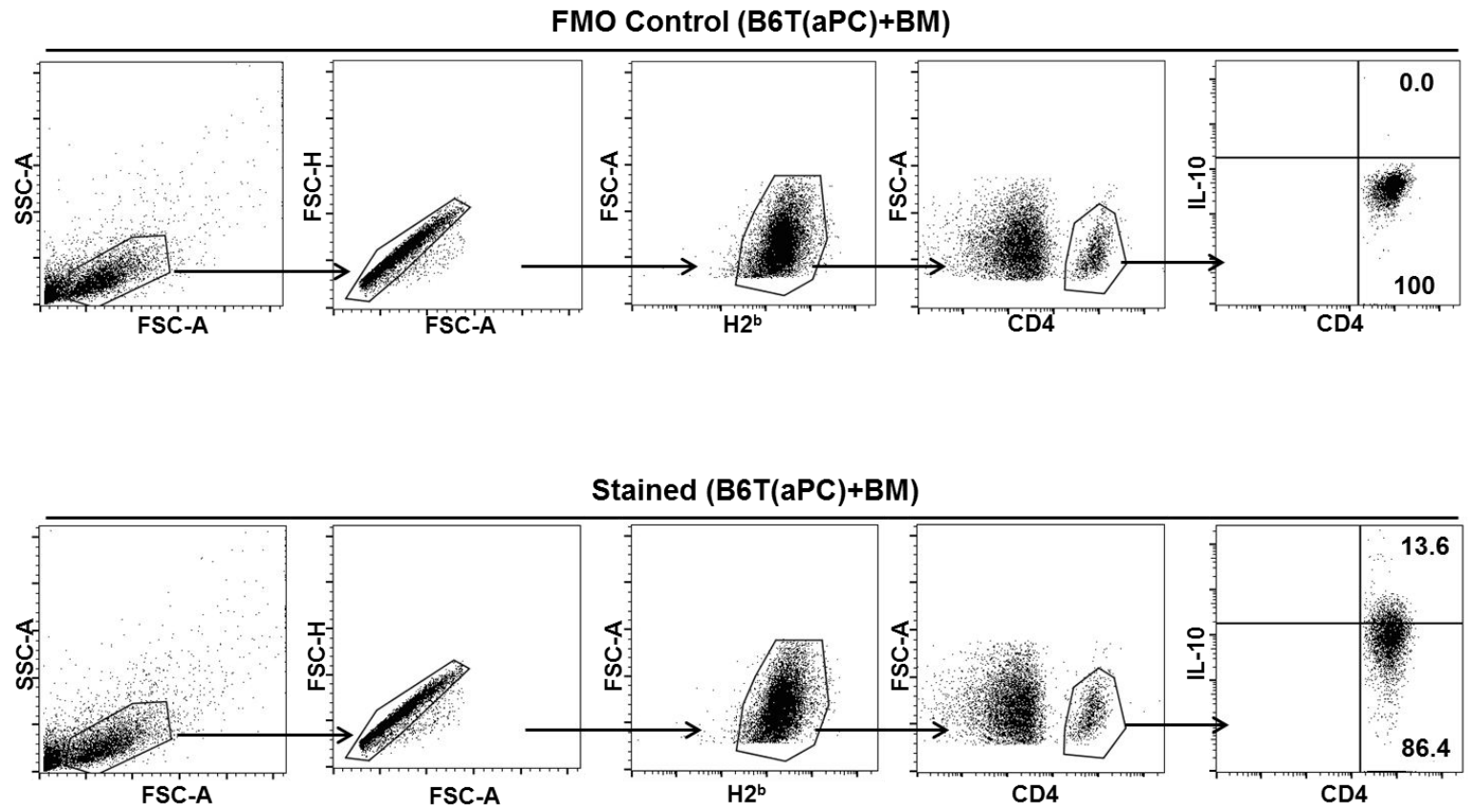


**Supplementary Fig. 19:** Representative gating strategy for FMO control and stained samples corresponding to Supplementary Figure 3.

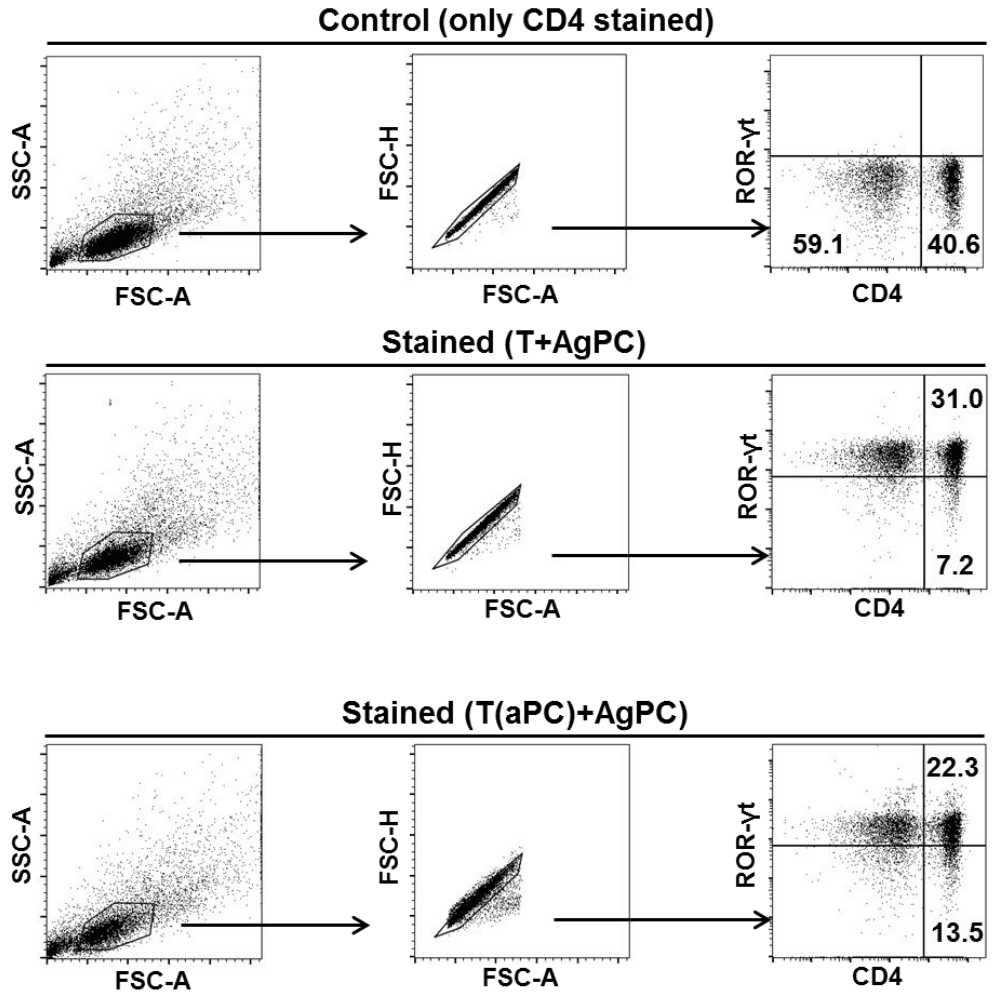


**Supplementary Fig. 20:** Representative gating strategy for control and stained samples corresponding to Supplementary Figure 6.

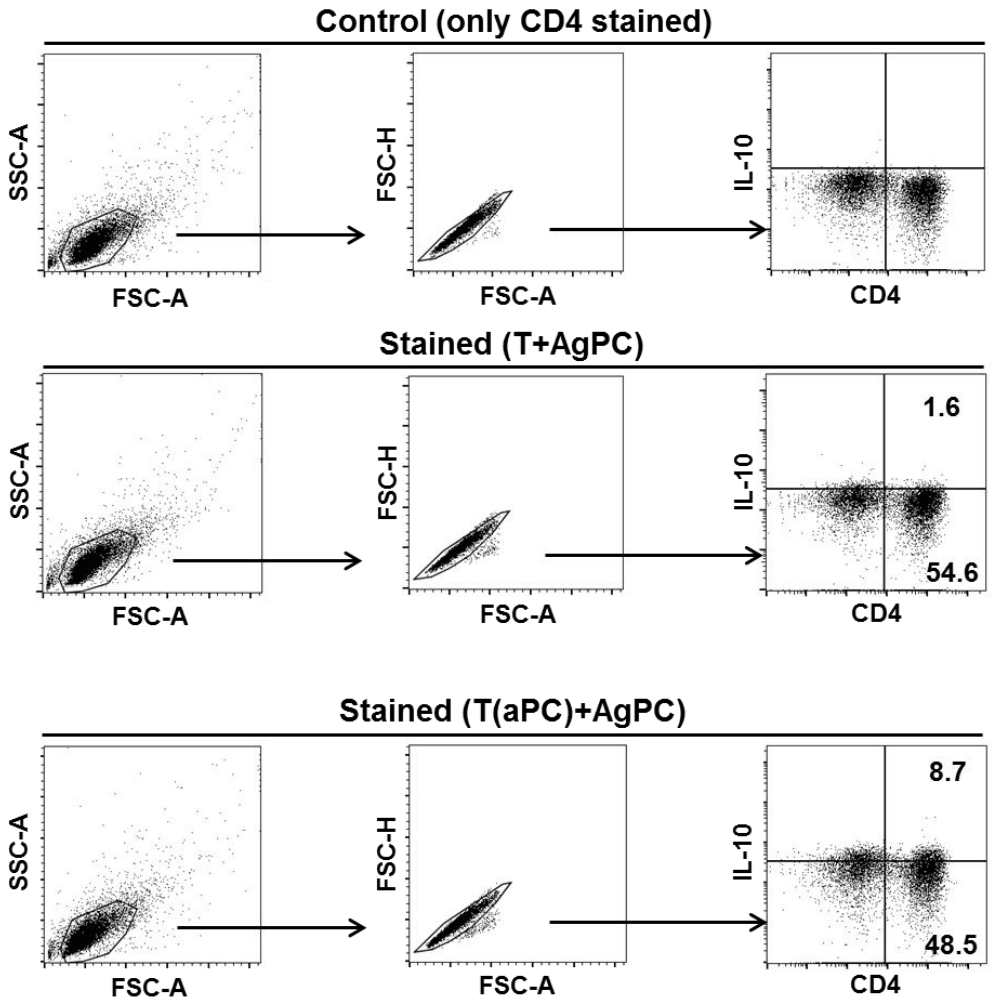


**Supplementary Fig. 21:** Representative gating strategy for control and stained samples corresponding to Supplementary Figure 7.

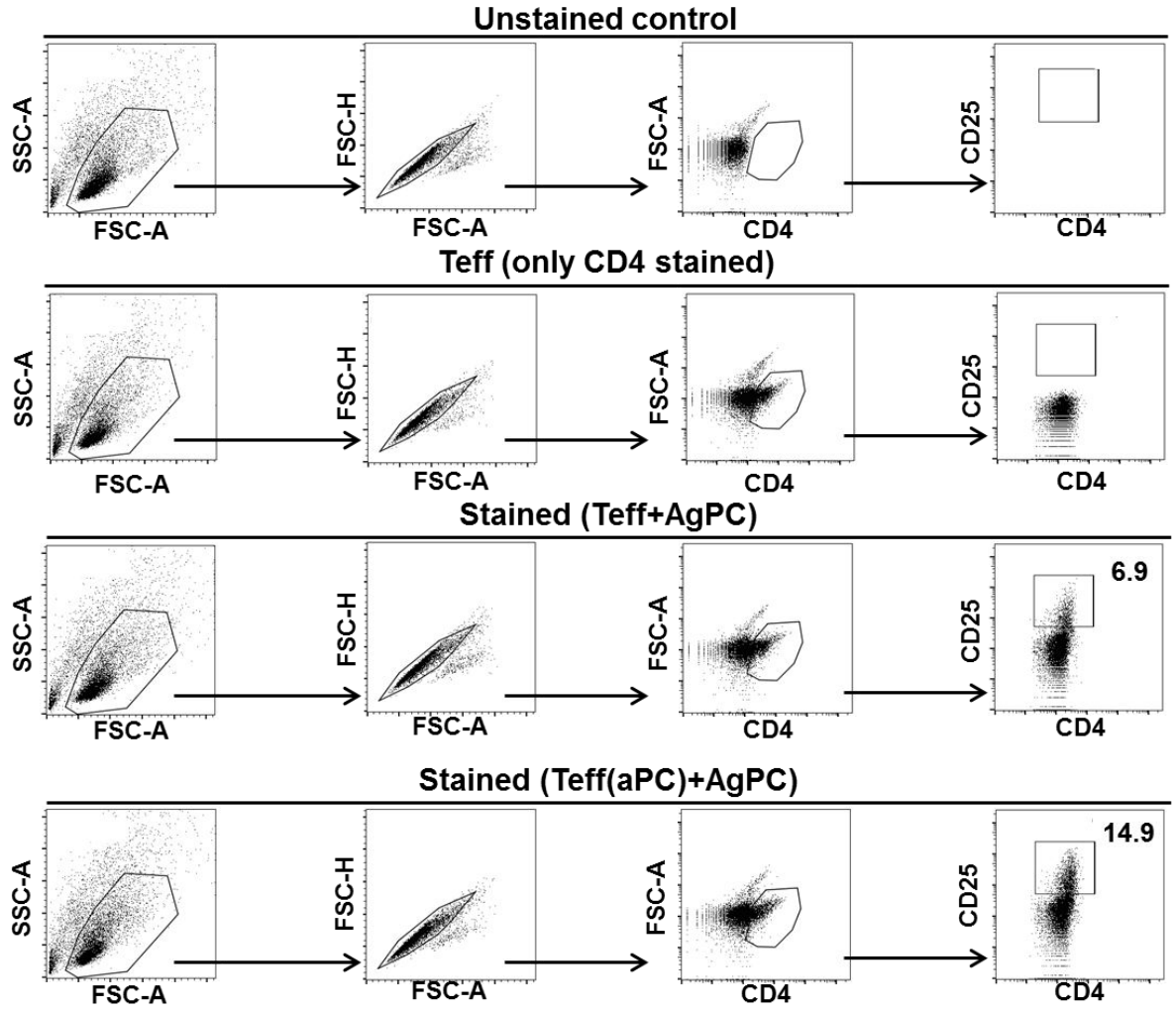


**Supplementary Fig. 22:** Representative gating strategy for control and stained samples corresponding to Supplementary Figure 10.

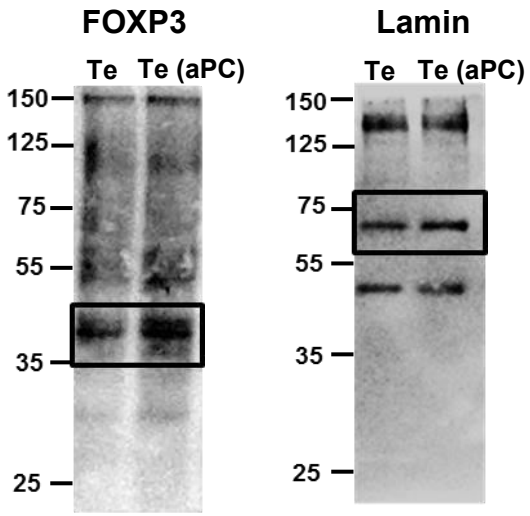


**Supplementary Fig. 23:** Full western blot images corresponding to Fig. 5f.

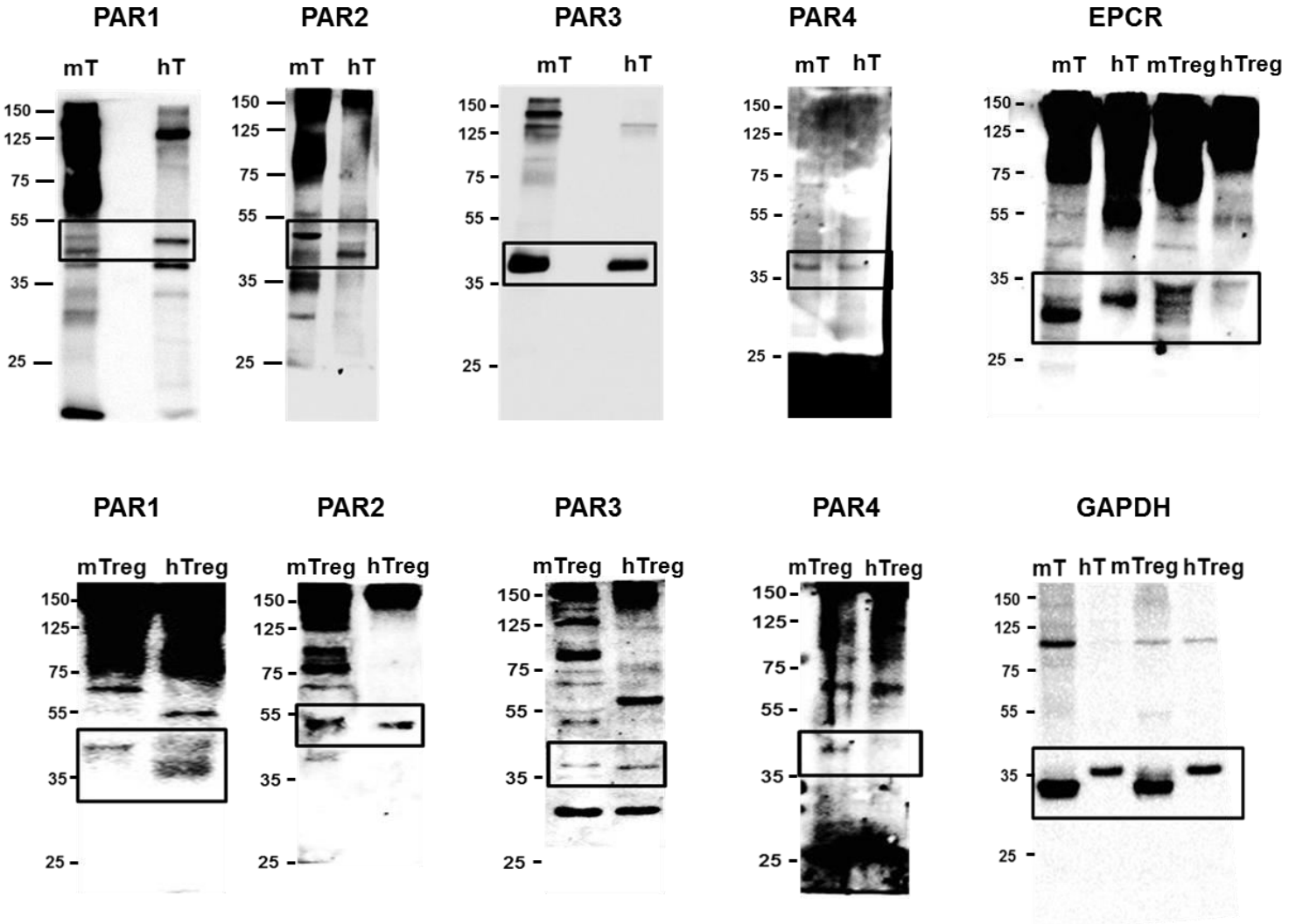


**Supplementary Fig. 24:** Full western blot images corresponding to Fig. 6a.

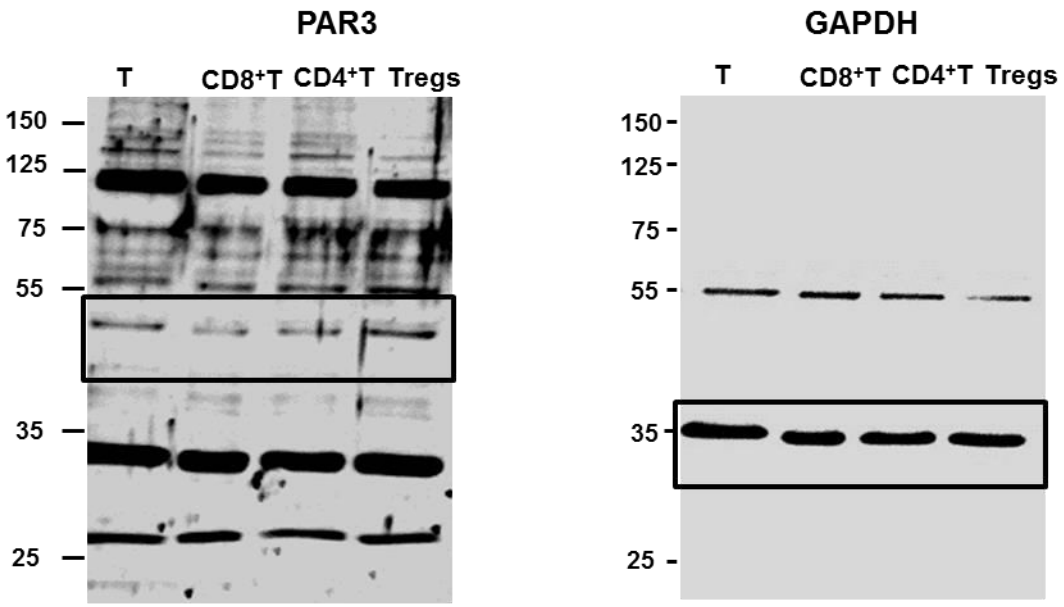


**Supplementary Fig. 25:** Full western blot images corresponding to Fig. 6b.

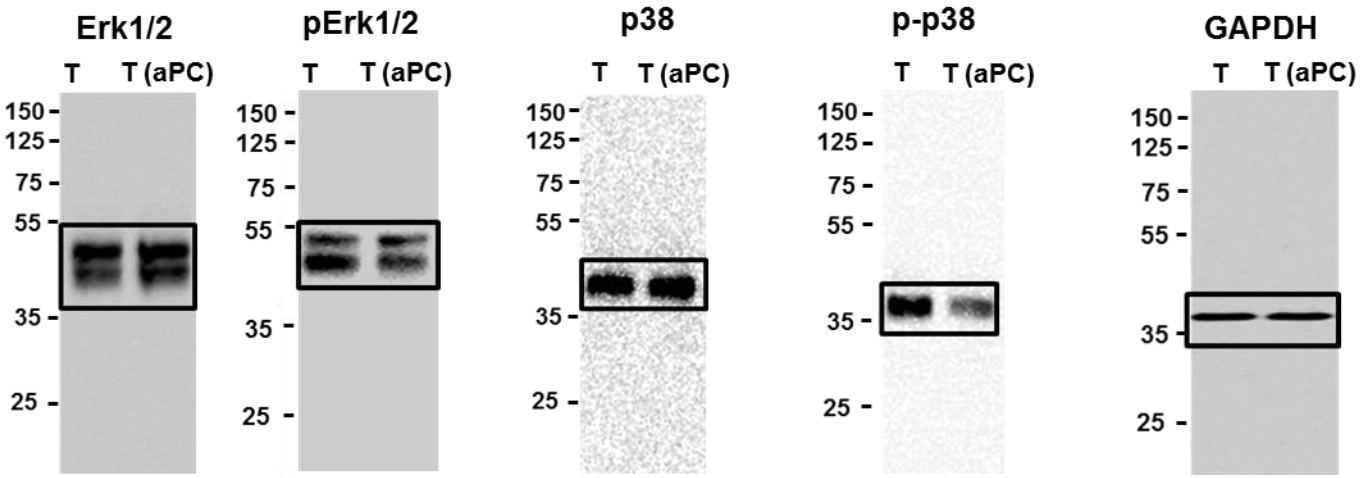


**Supplementary Fig. 26:** Full western blot images corresponding to Fig. 7c.

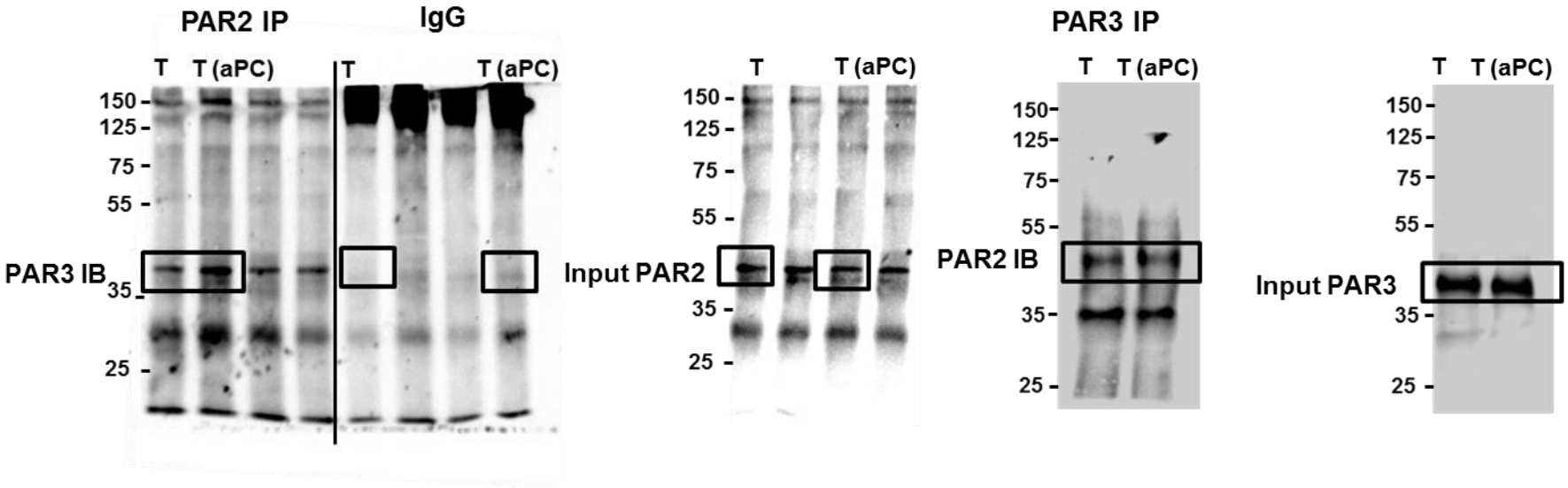


**Supplementary Fig. 27:** Full western blot images corresponding to Fig. 7d.

## Supplementary Table 1

| Antibody | Antibody Target | Clone | Host | Dilution | Source |
|---|---|---|---|---|---|
| H-2D$^b$-FITC | mouse MHC class I, H-2D^b | 28-14-8 | Mouse | 1:400 | eBioscience |
| H-2D$^b$-eFluor450 | mouse MHC class I, H-2D^b | 28-14-8 | Mouse | 1:400 | eBioscience |
| H-2K$^b$-FITC | mouse MHC class I, H-2Kd and H-2Dd | 34-1-2S | Mouse | 1:400 | eBioscience |
| CD4-FITC | human CD4 | OKT4 | Mouse | 1:400 | eBioscience |
| CD4-APC | mouse CD4 | RM4-5 | Rat | 1:1000 | Biolegend |
| FOXP3-PE | mouse FOXP3 | FJK-16S | Rat | 1:400 | eBioscience |
| FOXP3-PE-Cy7 | human FOXP3 | PCH101 | Rat | 1:400 | eBioscience |
| FOXP3-AlexaFluor647 | human, mouse FOXP3 | 150D | Mouse | 1:400 | BioLegend |
| T-bet-PE | mouse, human T-bet | 4B10 | Mouse | 1:200 | eBioscience |
| TNF-α-PE | mouse TNF-α | MP6-XT22 | Rat | 1:200 | eBioscience |
| IFN-γ-PE | mouse IFN-γ | XMG1.2 | Rat | 1:2000 | eBioscience |
| IL-10-PE | mouse IL-10 | JES5-16E3 | Rat | 1:200 | BioLegend |
| IL-17A-PE | mouse IL-17A | TC11-18H10 | Rat | 1:100 | BD |
| Ror-γt-PE | mouse Ror-γt | AFKJS-9 | Rat | 1:400 | eBioscience |
| T-bet-PerCp-Cy5.5 | mouse, human T-bet | 4B10 | Mouse | 1:1000 | eBioscience |
| TNF-α-PE | human TNF-α | MAb11 | Mouse | 1:200 | BioLegend |
| IFN-γ-PE | human IFN-γ | 4S.B3 | Mouse | 1:1000 | BioLegend |
| IL-10-PE | human IL-10 | JES3-19F1 | Rat | 1:200 | BioLegend |
| IL-17A-PE | human IL-17A | BL168 | Mouse | 1:200 | BioLegend |
| Ror-γt-PE | human, mouse Ror-γt | AFKJS-9 | Rat | 1:400 | eBioscience |
| FOXP3 | Full-length FOXP3 protein | 150D | Mouse | 1:1000 | BioLegend |
| PAR1 | human, mouse PAR1 | ATAP2 | Mouse | 1:200 | Santa Cruz |
| PAR2 | human, mouse PAR2 | SAM11 | Mouse | 1:200 | Santa Cruz |
| PAR3 | human, mouse PAR3 | H103 | Rabbit | 1:200 | Santa Cruz |
| PAR4 | human, mouse PAR4 | H120 | Rabbit | 1:200 | Santa Cruz |
| EPCR | human, mouse EPCR | RCR-252 | Rat | 1:500 | Sigma-Aldrich |
| Erk1/2 | human, mouse | Polyclonal | Rabbit | 1:1000 | Cell Signaling |
| Phospho-Erk1/2 | Thr202/Tyr204 human, mouse | Polyclonal | Rabbit | 1:1000 | Cell Signaling |
| p38 | human, mouse | Polyclonal | Rabbit | 1:1000 | Cell Signaling |
| Phospho-p38 | Thr180/Tyr182 | Polyclonal | Rabbit | 1:1000 | Cell Signaling |
| CD25-APC | human CD25 | BC96 | | 1:400 | BioLegend |
| CD3 | epsilon-subunit within the human CD3 complex | OKT3 | Mouse | 1µg/ml | eBioscience |
| CD28 | human CD28 molecule | CD28.2 | Mouse | 0.5µg/ml | eBioscience |
| GAPDH | Human, Mouse | Polyclonal | Rabbit | 1:20000 | Sigma-Aldrich |
| Anti-mouse IgG | Mouse IgG | | Horse | 1:2000 | Cell Signaling |
| Anti-rabbit IgG | Rabbit IgG | | Goat | 1:2000 | Cell Signaling |